University of Trento
Department of Physics
Bachelor's Degree in Physics

~ · ~

Academic Year 2021–2022

Geodesics in Schwarzschild Metric

Supervisor
Prof. Albino Perego

Graduate Student
Federico De Paoli
227552

Final examination date: September 2, 2024

Placeholder

Acknowledgments

Placeholder

Abstract

Devo fare l'abstract?

Contents

Introduction

Newtonian mechanics is built upon the concept of absolute time and space. Once the concept of *inertial frame* is introduced, physics can be done on a space described by Euclidean geometry. For inertial observers, free particles (particles on which no net forces are acting) move in a straight line, which is the shortest distance between two points in a three-dimensional space, measured as:

$$\Delta s^2 = \Delta x^2 + \Delta y^2 + \Delta z^2 \,. \tag{1}$$

On the other hand, time is *just* seen as a parameter, common to every inertial frame, that can be used to parametrize the trajectory and to determine the particle velocity and acceleration.

With the appearance of Maxwell's Equations it became clear that what they predicted (the speed of light being constant in every inertial frame) was in contrast with the description of our space given by Newtonian Mechanics, where the speed of anything changes with respect to the chosen inertial frame. Between Maxwell's Equations and Newtonian mechanics Einstein chose to modify the latter and wrote his two postulates for the theory of Special Relativity:

- The laws of physics are invariant (identical) in all inertial frames of reference;
- The speed of light in vacuum, $c = 299\,792\,458\text{m/s}$, is the same for all observers, regardless of the motion of light source or observer.

The postulates may or may not be intuitive, but simple observations based on them bring us to abandon the idea of absolute space and time and to introduce the concept of *spacetime*, together with a new way of measuring distances

$$\Delta s^2 = -c^2\Delta t^2 + \Delta x^2 + \Delta y^2 + \Delta z^2 \,. \tag{2}$$

In special relativity distances between events measured in this way are the same for every observer in every possible inertial frame.

The appearance of time in a formula that is supposed to give us the distance between two events is surely destabilizing at first, but geometry teaches us that fixing the way we calculate Δs^2, more properly referred to as the *line element* $\mathrm{d}s^2$, is enough to describe the geometry of the space that we are using. Since eq. 2 is different from eq. 1, in particular there is a minus sign in front of Δt^2, we moved away from the familiar three-dimensional Euclidean geometry and are now in four-dimensional spacetime, usually referred to as *flat spacetime* or *Minkowski space*.

This new geometry allowed for a reformulation of Maxwell's Equations and brought (and explained) phenomena like time dilation, length contraction and the relativity of simultaneity. The last one in particular, the concept that the simultaneity of two events depends on the frame of reference, poses a threat to the *force* of gravity. Up until this point gravity was defined as the instantaneous force F_{12} acting on a mass m_1 at time t due to a second mass m_2:

$$F_{12} = G\frac{m_1 m_2}{|r_1(t) - r_2(t)|^2} \tag{3}$$

The adjective *instantaneous* in a theory where nothing can travel faster than the speed of light should already raise some concern. But looking at $r_1(t)$ and $r_2(t)$ in eq. 3, that are supposed to indicate the positions of the masses in the same instant of time, makes it even clearer that the force F_{12} cannot be the same in all frames of reference.

Solving this issue gave birth to the theory of general relativity, where a mass is not a source of gravitational force anymore, but is responsible for bending the four-dimensional spacetime itself. This implies that when we observe a particle deviating its trajectory from a straight line in the presence of a massive object, it is not because of a force acting on it. In fact, we can consider the particle free and moving from point A to point B along the shortest path, it is just that in the curved surface bent by the mass the shortest path is not a straight line.

While this concept may not enhance our intuitive understanding, the implications and the mathematical formalism required to articulate the theory are even more challenging. If the presence of mass distorts the space we work in, changing the line element $\mathrm{d}s^2$ is therefore necessary. The details of the theories, particularly the Einstein field equations, that describe this distortion and allow us to evaluate the new $\mathrm{d}s$ from a give distribution of mass are beyond the scope of this thesis. Our focus will be on evaluating the observable effects, given the line element.

More specifically, we will study one of the simplest curved spacetimes that general relativity offers: a stationary, spherically symmetric spacetime. This geometry arises when the source of curvature is a spherical star but can also exist in the absence of any source. The latter case is associated with the presence of a black hole, with the corresponding solutions referred to as *black hole solutions*. It is one of the simplest because of the many symmetries that presents and, luckily, is also one of the most useful.

The line element of what is more commonly know as the Schwarzschild geometry is

$$\mathrm{d}s^2 = -\left(1 - \frac{2GM}{c^2 r}\right)(c\mathrm{d}t)^2 + \left(1 - \frac{2GM}{c^2 r}\right)^{-1}\mathrm{d}r^2 + r^2(\mathrm{d}\theta^2 + \sin^2\theta\mathrm{d}\phi^2) \tag{4}$$

expressed in spherical coordinates centered in the mass responsible for bending the space.

To explore this geometry, we will examine the possible trajectories of both a free particle and a photon. By analyzing the paths of particles with varying energies and directions as they move around the massive object, we can gain insight into some of the implications of the Schwarzschild metric.

Chapter 1

Theory

The content of this chapter is mostly based on **hartle2021gravity** *and* **shapiro2008black**.

1.1 Notation and Formalism

In the *flat spacetime* we can introduce a coordinate basis for four-vectors

$$\mathbf{e_t} = (1,0,0,0), \quad \mathbf{e_y} = (0,1,0,0), \quad \mathbf{e_y} = (0,0,1,0), \quad \mathbf{e_z} = (0,0,0,1). \tag{1.1}$$

The set $\{\mathbf{e_t}, \mathbf{e_x}, \mathbf{e_y}, \mathbf{e_z}\}$, is often referred to as $\{\mathbf{e_0}, \mathbf{e_1}, \mathbf{e_2}, \mathbf{e_3}\}$. Any four-vector $\mathbf{a}$ can then be written as

$$\mathbf{a} = a^t\mathbf{e_t} + a^x\mathbf{e_x} + a^y\mathbf{e_y} + a^z\mathbf{e_z} = a^0\mathbf{e_0} + a^1\mathbf{e_1} + a^2\mathbf{e_2} + a^3\mathbf{e_3} \tag{1.2}$$

where $(a_t,\ a_x,\ a_y,\ a_z)$, or equivalently $(a_0,\ a_1,\ a_2,\ a_3)$, are the components of the four-vector.

Another useful convention is to use Roman letters (usually i or j) to refer to indices 1, 2, 3 and Greek letters (usually μ or ν) to refer to indices 0, 1, 2, 3. Using Einstein notation the expression in eq. 1.2, can be rewritten simply as $\mathbf{a} = a^\mu\mathbf{e}_\mu$. Other useful ways to specify the components of $\mathbf{a}$ are

$$a^\mu = (a^t, a^x, a^y, a^z) \quad a^\mu = (a^t, a^i) \quad a^\mu = (a^t, \vec{a})$$

where $\vec{a} = a^i e_i$ is the tree-dimensional vector (a_x, a_y, a_z).

The length of the four-vector $\mathbf{a}$ must be evaluated using the line element of the flat spacetime, described in eq. 2. In general, a useful way to do that is by first defining the *metric* $\eta_{\nu\mu}$

$$\eta_{\nu\mu} = \begin{array}{c} \\ t \\ x \\ y \\ z \end{array} \begin{array}{c} \begin{array}{cccc} t & x & y & z \end{array} \\ \begin{pmatrix} -1 & 0 & 0 & 0 \\ 0 & 1 & 0 & 0 \\ 0 & 0 & 1 & 0 \\ 0 & 0 & 0 & 1 \end{pmatrix} \end{array} \qquad \Longrightarrow \qquad \mathrm{d}s^2 = \eta_{\nu\mu}\mathrm{d}x^\nu\mathrm{d}x^\mu \tag{1.3}$$

Here the double sum is implied, and we rightfully notice that the minus sign has appeared again under the t component. Now we can compactly write

$$\mathbf{a}\cdot\mathbf{a} = \eta_{\mu\nu}\, a^\mu\, a^\nu = -(a^t)^2 + (a^x)^2 + (a^y)^2 + (a^z)^2 \tag{1.4}$$

Without any claim of rigorously demonstrating it, we can say that since this scalar product is built from the line element $\mathrm{d}s^2$, it is the same in every inertial frame one might choose. Quantities that have these properties are *invariant*.

When working in the Schwarzschild geometry it is useful to adopt the Schwarzschild coordinates: spherical coordinates centered at the center of the mass M. Instead of describing a four-vector with the components $(a_t,\ a_x,\ a_y,\ a_z)$, we will use $(a_t,\ a_r,\ a_\theta,\ a_\phi)$.

Given the expression of the line element in eq. 4 it is useful to adopt geometrized units, where $G = c = 1$ (Appendix A). From now on we will always use geometrized units (referring to them as $\mathcal{L}$) unless stated otherwise. The line element and the metric can be rewritten as

$$\mathrm{d}s^2 = -\left(1 - \frac{2M}{r}\right)(\mathrm{d}t)^2 + \left(1 - \frac{2M}{r}\right)^{-1}\mathrm{d}r^2 + r^2(\mathrm{d}\theta^2 + \sin^2\theta\mathrm{d}\phi^2) \tag{1.5}$$

$$g_{\nu\mu} = \begin{array}{c} \\ t \\ r \\ \theta \\ \phi \end{array} \begin{array}{c} \begin{array}{cccc} t & r & \theta & \phi \end{array} \\ \begin{pmatrix} -(1-2M/r) & 0 & 0 & 0 \\ 0 & (1-2M/r)^{-1} & 0 & 0 \\ 0 & 0 & r^2 & 0 \\ 0 & 0 & 0 & r^2\sin^2\theta \end{pmatrix} \end{array} . \tag{1.6}$$

It is worth pointing out that, given 1.5 and 1.6, when we introduce this coordinate frame

$$\mathbf{e_t} = (1,\ 0,\ 0,\ 0) \quad \mathbf{e_r} = (0,\ 1,\ 0,\ 0) \quad \mathbf{e}_\theta = (0,\ 0,\ 1,\ 0) \quad \mathbf{e}_\phi = (0,\ 0,\ 0,\ 1) \tag{1.7}$$

it has the inconvenience of not being normalized. For example

$$\mathbf{e_t} \cdot \mathbf{e_t} = g_{\nu\mu} e_t^\mu e_t^\nu = g_{00} = -(1 - 2M/r)\,. \tag{1.8}$$

If we want an orthonormal tetrad we can define

$$\hat{\mathbf{e}}_\mathbf{t} = \left(1 - \frac{2M}{r}\right)^{-1/2}\mathbf{e_t} \qquad \Longrightarrow \qquad \hat{\mathbf{e}}_\mathbf{t} \cdot \hat{\mathbf{e}}_\mathbf{t} = g_{\nu\mu}\hat{e}_t^\mu \hat{e}_t^\nu = g_{00}\left(1 - \frac{2M}{r}\right)^{-1} = -1 \tag{1.9a}$$

$$\hat{\mathbf{e}}_\mathbf{r} = \left(1 - \frac{2M}{r}\right)^{1/2}\mathbf{e_r} \qquad \Longrightarrow \qquad \hat{\mathbf{e}}_\mathbf{r} \cdot \hat{\mathbf{e}}_\mathbf{r} = g_{\nu\mu}\hat{e}_r^\mu \hat{e}_r^\nu = g_{00}\left(1 - \frac{2M}{r}\right) = 1 \tag{1.9b}$$

$$\hat{\mathbf{e}}_\theta = \frac{1}{r}\mathbf{e_t} \qquad \Longrightarrow \qquad \hat{\mathbf{e}}_\theta \cdot \hat{\mathbf{e}}_\theta = 1 \tag{1.9c}$$

$$\hat{\mathbf{e}}_\phi = \frac{1}{r\sin\theta}\mathbf{e_t} \qquad \Longrightarrow \qquad \hat{\mathbf{e}}_\phi \cdot \hat{\mathbf{e}}_\phi = 1 \tag{1.9d}$$

1.2 Proprieties of the Metric

Let's first analyze the Schwarzschild metric in more detail:

$$\mathrm{d}s^2 = -\left(1-\frac{2M}{r}\right)(\mathrm{d}t)^2 + \left(1-\frac{2M}{r}\right)^{-1}\mathrm{d}r^2 + r^2(\mathrm{d}\theta^2+\sin^2\theta\mathrm{d}\phi^2) \tag{1.10}$$

There are two singularities in $r=0$ and $r=2M$. The first one is a true, physical singularity, since the spacetime curvature diverges for $r\to 0$. The second one is a coordinate singularity and occurs at what is defined as the Schwarzschild $r_s = 2M$. Every non-black hole object has a radius larger than its Schwarzschild radius. The nature and significance of this will become clearer in the subsequent sections.

On the other hand, if we take the limit as r approaches infinity, we notice that the metric becomes asymptotically flat, approaching the metric of Minkowski space. Therefore, we can refer to the value a quantity would have at a great distance to find a more familiar expression.

Finally, $\mathrm{d}s^2$ is independent of the coordinates t and ϕ. This is expected, as the mass responsible for curving the spacetime is static and spherically symmetric or in the case of a black hole solution, the spacetime is spherical and stationary (Birkhoff's theorem guarantees that if the metric is spherically symmetric and static, then it is also stationary). The metric independence from time and rotation implies the existence of two, easy to find, *Killing vectors*:

$$\xi = (1,0,0,0) \quad \text{and} \quad \eta = (0,0,0,1)\,. \tag{1.11}$$

A *killing vector* is a direction in the four-dimensional spacetime along which we can freely move without changing the metric. It is a general way to describe a symmetry of the metric. Since symmetries correspond to conserved quantities they will be a key point in studying the trajectories of free particles and photons.

We start by considering the four-momentum $\mathbf{p}$ of a particle of mass m, defined as

$$p^\mu := mu^\mu = m\frac{\mathrm{d}x^\mu}{\mathrm{d}\tau} \tag{1.12}$$

where u is the four-velocity of the particle, x a four-vector describing its position and τ the proper time. Therefore, for a free particle, the quantities

$$E = -\xi\cdot\mathbf{p} = -g_{00}\,p^0 = m\left(1-\frac{2M}{r}\right)\frac{\mathrm{d}x^t}{\mathrm{d}\tau}$$

$$L = \eta\cdot\mathbf{p} = g_{33}\,p^\phi = mr^2\sin^2\theta\frac{\mathrm{d}x^\phi}{\mathrm{d}\tau}$$

will be conserved during the motion. We already named them E and L as they are respectively the energy and the angular momentum at large r and low velocities. To simplify the expressions used in the discussion will use normalized quantities

$$e := \frac{E}{m} = \left(1-\frac{2M}{r}\right)\frac{\mathrm{d}x^t}{\mathrm{d}\tau} \tag{1.13a}$$

$$\ell := \frac{L}{m} = r^2\sin^2\theta\frac{\mathrm{d}x^\phi}{\mathrm{d}\tau}\,. \tag{1.13b}$$

e and ℓ are respectively the conserved energy and angular momentum per unit rest mass.

For a massless particle (e.g. a photon) the proper time can not be used, so the four-velocity can be defined using an *affine parameter* λ.

$$u^\mu = \frac{\mathrm{d}x^\mu}{\mathrm{d}\lambda} \tag{1.14}$$

We can define the conserved quantities e and l in the same way, using the four-velocity

$$e := -\xi \cdot \mathbf{u} = \left(1 - \frac{2M}{r}\right) \frac{\mathrm{d}x^t}{\mathrm{d}\lambda} \tag{1.15a}$$

$$\ell := \eta \cdot \mathbf{u} = r^2 \sin^2\theta \frac{\mathrm{d}x^\phi}{\mathrm{d}\lambda}\,. \tag{1.15b}$$

getting the same result except for having λ instead of τ.
In the next sections the normalization of the four-velocity $\mathbf{u}$ will be really useful too

$$\mathbf{u}\cdot\mathbf{u} = g_{\nu\mu}u^\nu u^\mu = -1 \qquad \text{for } m \neq 0 \tag{1.16a}$$

$$\mathbf{u}\cdot\mathbf{u} = g_{\nu\mu}u^\nu u^\mu = 0 \qquad \text{for } m = 0\,. \tag{1.16b}$$

It is not just a property of the metric, but it is valid for every $g_{\nu\mu}$. Equations 1.16a and 1.16b can be respectively derived in this way:

$$g_{\nu\mu}\mathrm{d}x^\nu \mathrm{d}x^\mu = \mathrm{d}s^2 \quad \Longrightarrow \quad g_{\nu\mu}\frac{\mathrm{d}x^\nu}{\mathrm{d}\tau}\frac{\mathrm{d}x^\mu}{\mathrm{d}\tau} = \frac{\mathrm{d}s^2}{\mathrm{d}\tau^2} \quad \Longrightarrow \quad \mathbf{u}\cdot\mathbf{u} = -1 \tag{1.17a}$$

$$g_{\nu\mu}\mathrm{d}x^\nu \mathrm{d}x^\mu = \mathrm{d}s^2 \quad \Longrightarrow \quad g_{\nu\mu}\frac{\mathrm{d}x^\nu}{\mathrm{d}\lambda}\frac{\mathrm{d}x^\mu}{\mathrm{d}\lambda} = 0 \quad \Longrightarrow \quad \mathbf{u}\cdot\mathbf{u} = 0 \tag{1.17b}$$

Using the definition of proper time $\mathrm{d}\tau^2 = -\mathrm{d}s^2$ in 1.17a and the property of the light rays $\mathrm{d}s^2 = 0$ in 1.17b.

1.3 Gravitational Redshift

Let's consider a static observer in r. When an observer measures the energy of a photon, that corresponds to the t component of the four-momentum of the photon, $\mathbf{p}$, they do that using their local orthonormal tetrad that we described in 1.9.

Referring to $p^{\hat{t}}$ as the value measured in the orthonormal tetrad $\{\hat{\mathbf{e}}_\mathbf{t}, \hat{\mathbf{e}}_\mathbf{r}, \hat{\mathbf{e}}_\theta, \hat{\mathbf{e}}_\phi\}$ and p^t as the value measured with the coordinate basis $\{\mathbf{e_t}, \mathbf{e_r}, \mathbf{e}_\theta, \mathbf{e}_\phi\}$, the energy measured in r will be

$$E(r) = p^{\hat{t}} = \mathbf{p}\cdot\hat{\mathbf{e}}_\mathbf{t} = \mathbf{p}\cdot\mathbf{e_t}\left(1 - \frac{2M}{r}\right)^{-1/2} = \mathbf{p}\cdot\xi\left(1 - \frac{2M}{r}\right)^{-1/2}$$

$$\left(1 - \frac{2M}{r}\right)^{1/2} E(r) = \mathbf{p}\cdot\xi = \text{const}\,. \tag{1.18}$$

Where we used the expression for $\hat{e}_t$ from eq. 1.9a and notice that $\mathbf{e_t} = \xi$ from eq. 1.1 and eq. 1.11. Solving for the constant $\mathbf{p}\cdot\xi$ we find the expression in 1.18. The relationship between the energy of a photon measured at r' and the one measured at r from two static observers using their own tetrad is

$$\left(1 - \frac{2M}{r'}\right)^{1/2} E(r') = \left(1 - \frac{2M}{r}\right)^{1/2} E(r)$$

Taking the limit as r' approaches infinity and using $E = \hbar\omega$ for the energy of the photon

$$\omega_\infty = \omega_* \left(1 - \frac{2M}{r}\right)^{1/2} . \tag{1.19}$$

Here, ω_∞ is the frequency measured by a distant observer at $r \gg r_s$, while w_* denotes the frequency measured at a specific distance r. Photons observed at a certain distance from a star exhibit a lower frequency compared to the one they have at the point of emission.

1.4 Particle Orbits

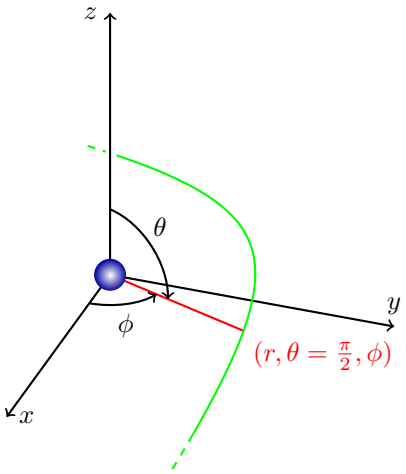

Figure 1.1: Visual representation of the spherical coordinates used. The green line represents a possible trajectory on the xy plane.

To further analyze the Schwarzschild geometry, we will now explore the behavior of a test particle within it. The term *test particle* refers to an object with mass so small that its influence on the surrounding spacetime is negligible, allowing us to analyze its motion without altering the geometry of the spacetime itself.
As already established from eq. 1.13b the angular momentum is conserved during the motion of a particle in this geometry. This implies that the particle's orbit must lie within a plane. Without loosing generality we can imagine the particle path to stay in the xy plane, fixing $\theta = \pi/2$ and, consequently,

$$u^\theta = \frac{\mathrm{d}\theta}{\mathrm{d}\tau} = 0$$

$$\ell = r^2 \sin^2\theta \frac{\mathrm{d}\phi}{\mathrm{d}\tau} = r^2 \frac{\mathrm{d}\phi}{\mathrm{d}\tau}$$

Refer to Figure 1.1 for a visual representation.

The four-velocity of our test particle can then be written as

$$u^\mu = \left(\frac{\mathrm{d}x^t}{\mathrm{d}\tau}, \frac{\mathrm{d}x^r}{\mathrm{d}\tau}, \frac{\mathrm{d}x^\theta}{\mathrm{d}\tau}, \frac{\mathrm{d}x^\phi}{\mathrm{d}\tau}\right) = \left(e\left(1 - \frac{2M}{r}\right)^{-1}, \frac{\mathrm{d}r}{\mathrm{d}\tau}, 0, \frac{\ell}{r^2}\right) .$$

Where we simplified the notation using $r = x^r$ and eliminated the dependence from x^t and x^ϕ using the conserved quantities e (eq. 1.13a) and ℓ (eq. 1.13b) respectively. Thanks to the normalization of $\mathbf{u}$ (eq. 1.16a) and using $\theta = \pi/2$ again, we can write

$$-1 = g_{\nu\mu} u^\nu u^\mu = -\left(1 - \frac{2M}{r}\right)^{-1} e^2 + \left(1 - \frac{2M}{r}\right)^{-1} \left(\frac{\mathrm{d}r}{\mathrm{d}\tau}\right)^2 + \frac{\ell^2}{r^2} .$$

Rearranging the expression, we have

$$e^2 = \left(\frac{\mathrm{d}r}{\mathrm{d}\tau}\right)^2 + \left(1 + \frac{\ell^2}{r^2}\right)\left(1 - \frac{2M}{r}\right) . \tag{1.20}$$

To compare eq. 1.20 with the Newtonian case we can expand the product, subtract 1 from both sides and divide by a factor of 2:

$$\mathcal{E} := \frac{e^2 - 1}{2} = \frac{1}{2}\left(\frac{\mathrm{d}r}{\mathrm{d}\tau}\right)^2 + \frac{\ell^2}{2r^2} - \frac{M}{r} - \frac{M\ell^2}{r^3}\,. \tag{1.21}$$

By defining this dimensionless constant $\mathcal{E}$, we can now see the derivative of r as the kinetic energy (per unit rest mass) and the other terms as an effective potential acting on the particle, defined as

$$V_{\text{eff}}(r) := \frac{\ell^2}{2r^2} - \frac{M}{r} - \frac{M\ell^2}{r^3}\,. \tag{1.22}$$

To better understand eq. 1.22, we can express it in $\mathcal{LMT}$ units, substituting $\ell \to \ell/c$ and $M \to GM/c^2$

$$V_{\text{eff}}(r) = \frac{1}{c^2}\left(\frac{\ell^2}{2r^2} - \frac{GM}{r} - \frac{GM\ell^2}{c^2 r^3}\right)$$

The first two terms are identical to the Newtonian potential for a particle with angular momentum (per mass) ℓ, orbiting around an object of mass M. The third one is new, negligible for $GM\ell^2 \ll c^2 r^3$, and it is proportional to r^{-3}.

Figure 1.2 shows the effect of the r^{-3} term: the infinite centrifugal barrier of the Newtonian potential disappears in V_{eff} and a particle with enough energy can fall to the center of the massive object.

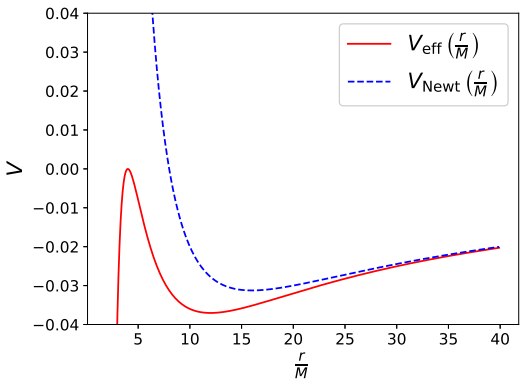

Figure 1.2: Effective potential defined in eq. 1.22 against the Newtonian potential, $\ell/M = 4$. The r^{-3} term dominates for $r \sim r_s$ and the particle can fall into the massive object. On the other hand the Newtonian potential presents its characteristic infinite centrifugal barrier.

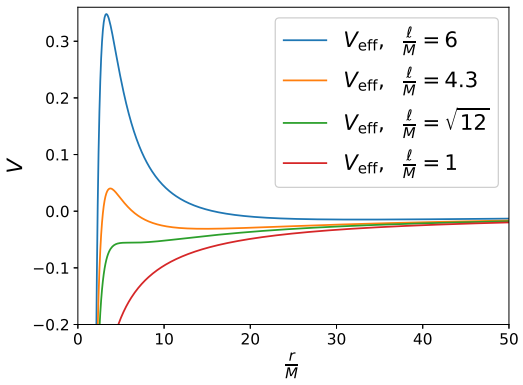

Figure 1.3: V_{eff} for different values of ℓ/M. For $\ell/M = \sqrt{12}$ (green) we can see r_{ISCO} the limit of the smallest stable orbit (eq. 1.23b. For $\ell/M = 1$ (red) there is no stationary point. The only stable points can be found for $\ell/M > \sqrt{12}$, in r_+, defined in eq. 1.23a.

By Taking the derivative of V_{eff} with respect to r we can predict the existence of stationary points for $\frac{\ell}{M} \geq \sqrt{12}$.

$$r_{+/-} = \frac{\ell^2}{2M}\left[1 \pm \sqrt{1 - 12\left(\frac{M}{\ell}\right)^2}\right] \qquad \frac{\ell}{M} > \sqrt{12} \tag{1.23a}$$

$$r_{\text{ISCO}} = 6M \qquad \frac{\ell}{M} = \sqrt{12} \tag{1.23b}$$

In eq. 1.23a r_- and r_+ correspond to an unstable point and to a stable one respectively.

The case described by eq. 1.23b represents the *innermost stable circular orbit* (ISCO). As the name suggests, it is the limit of the smallest stable orbit that a particle can theoretically follow. It is shown in green in Figure 1.3.

For $\frac{\ell}{M} < \sqrt{12}$ there are no stationary points and the particle either escapes to infinity or falls towards the mass M (red line in Figure 1.3).

As in the Newtonian case a bound orbit exists only when V_{eff} has a stable stationary point and the total energy given to the particle is not greater than $V_{\text{eff}}(r_-)$ (a more detailed explanation will be given in Section 1.6).

1.5 The Simplest Geodesics: Radial Infalls

The simplest case of particle we can consider is a radial infall where ϕ stays constant. From eq. 1.13b this implies $\ell = 0$.

Eq. 1.20 becomes

$$e^2 = \left(\frac{\mathrm{d}r}{\mathrm{d}\tau}\right)^2 + 1 - \frac{2M}{r}$$

$$\frac{\mathrm{d}r}{\mathrm{d}\tau} = -\sqrt{e^2 - 1 + \frac{2M}{r}}\,. \tag{1.24}$$

Where we chose the negative root as we want to discuss the case where the radius is decreasing. Looking at the parameter e in eq. 1.24 we can distinguish 3 cases:

- $e^2 < 1$: the particle has to start from a finite radius $r = R$ for the argument of the square root to be positive;
- $e = 1$: the particle starts at rest from $r = \infty$ (that implies $\frac{\mathrm{d}t}{\mathrm{d}\tau} = 1$ at infinity and $e = 1$ from eq. 1.13a);
- $e^2 > 1$: the particle starts from $r = \infty$ and also has some inward velocity.

We choose to analyze the case where $e = 1$ because it allows to easily solve eq. 1.24 analytically. We get

$$\frac{\mathrm{d}r}{\mathrm{d}\tau} = -\sqrt{\frac{2M}{r}}\,. \tag{1.25}$$

$$r^{1/2}\mathrm{d}r = -(2M)^{1/2}\mathrm{d}\tau$$

$$r(\tau) = \left(\frac{3}{2}\right)^{2/3} (2M)^{1/3}(\tau_* - \tau)^{2/3}\,. \tag{1.26}$$

Where τ_* is an integration constant that fixes the proper time τ when the particle arrives at $r = 0$. An observer that falls together with the particle will measure a finite time when he reaches $r = 2M$ and $\tau = \tau_*$ at $r = 0$.

On the contrary the experience of an observer far away from the source of curvature, that measures the Schwarzschild time t it is much different. To see this we can solve eq. 1.25 with respect to t. Using the chain rule to derive r with respect to t and eliminating the dependence from τ using eq. 1.13a with $e = 1$, we get

$$-\sqrt{\frac{2M}{r}} = \frac{\mathrm{d}r}{\mathrm{d}\tau} = \frac{\mathrm{d}t}{\mathrm{d}\tau}\frac{\mathrm{d}r}{\mathrm{d}t} = \left(1 - \frac{2M}{r}\right)^{-1}\frac{\mathrm{d}r}{\mathrm{d}t}$$

$$\frac{\mathrm{d}t}{\mathrm{d}r} = -\left(\frac{2M}{r}\right)^{-1/2}\left(1 - \frac{2M}{r}\right)^{-1}$$

The integration is not as immediate as the previous one, but can be resolved by substituting $u = \sqrt{r}$ and then by breaking the fraction into simpler ones repeatedly. The result, fixing a similar time constant t_* as before, is

$$t = t_* + 2M\left[-\frac{3}{2}\left(\frac{r}{2M}\right)^{3/2} - 2\left(\frac{r}{2M}\right)^{1/2} + \ln\left|\frac{(r/2M)^{1/2}+1}{(r/2M)^{1/2}-1}\right|\right] . \tag{1.27}$$

We can not find $r(t)$ analytically as was done previously, but the expression in 1.27 already tells us that for $r \to 2M$ the time measured by a far observer goes to infinity. This implies that the distant observer will never see the particle reaching $r = 2M$ and entering the Schwarzschild radius, they will only see it getting closer and closer forever.
If the particle is emitting a signal with a frequency w_*, they will measure it infinitely redshifted as described by eq. 1.19, asymptotically going to $\omega_\infty = 0$. That is why the Schwarzschild radius is also referred to as a *source of infinite redshift*.
Figure 1.4 shows eq. 1.26 and eq 1.27, the integration constants τ_* and t_* where chosen to make both equations start from the same point $r \simeq 12M$ at $\tau = t = 0$.

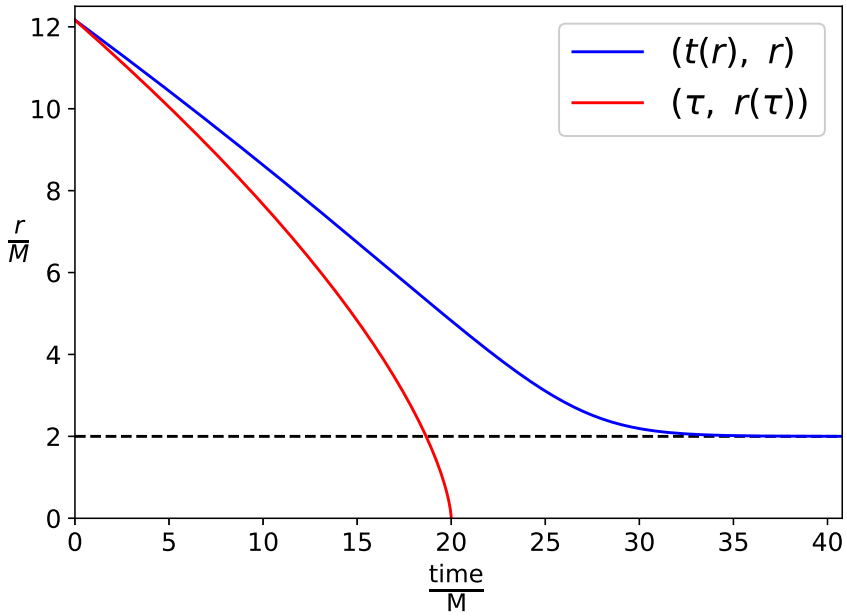

Figure 1.4: Eq. 1.26 and eq. 1.27 describing the fall from $r \simeq 12M$ on. The integration constants τ_* and t_* where fixed so that both equations started from the same $r(0)$. $r(\tau)$ gets to 0 quickly (at $\tau = \tau_*$), while $t(r)$ goes to infinity for $r \to r_s = 2M$. The Schwarzschild radius r_s is represented with the dashed black line.

1.6 Stable Orbits

In Section 1.4 we analyzed the role that $\frac{\ell}{M}$ has on the effective potential V_{eff} defined in eq. 1.22 and found out that for $\frac{\ell}{M} > \sqrt{12}$ it has two stationary points $r_{+/-}$ defined in eq. 1.23a.

For clarity, we rewrite eq. 1.21 below, accompanied by a visual representation in Figure 1.5.

$$\left(\frac{\mathrm{d}r}{\mathrm{d}\tau}\right)^2 = \mathcal{E} - V_{\text{eff}}(r) \tag{1.28}$$

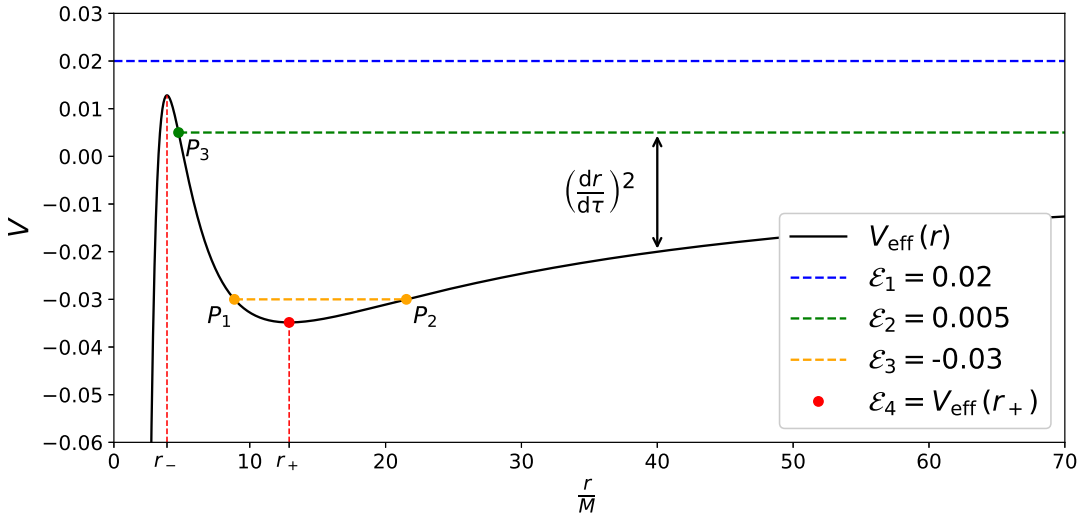

Figure 1.5: In black the effective potential with $\ell/M = 4.1$. The dashed horizontal lines, along with the red dot, represent possible values of $\mathcal{E}$ that give 4 different scenarios. Refer to the text for a detailed explanation.
This figure is inspired by **shapiro2008black**.

From eq. 1.28 we know that the particle can change its distance r from the massive object only if there is the energy $\mathcal{E} - V_{\text{eff}}$ to do so. In Figure 1.5, V_{eff} with $\ell/M = 4.1$ is represented along with 4 different values of $\mathcal{E}$.

The red full dot represents the case where the particle has exactly the energy required to stay in the local minimum of the potential. Here there is no *spare* energy that the particle can use to move along r. This is the case of a circular orbit, and it will be explored in Section 1.6.1

In the yellow case, $\mathcal{E} = -0.03$, the particle has some *spare* energy (not enough to escape) to change its radius between the two turning points P_1 and P_2. This results in an ellipse-like shape around the massive object. [1]

Finally, the green case, $\mathcal{E} = 0.005$, and the blue one, $\mathcal{E} = 0.02$, are not stable orbits. In the first case, the particle has one turning point P_3 and has enough energy to escape the potential well on the right and go back towards infinity. In the latter, the particle as a bigger energy than $V_{\text{eff}}(r_-)$ and can fall into the massive object, if u^r is directed inward.

[1] As we will see in Section 1.6.2 it is not exactly an ellipse as in the Newtonian case.

1.6.1 Circular Orbits

As we have seen from Figure 1.5 a particle can draw a perfectly circular orbit if it has an energy $\mathcal{E} = V_{\text{eff}}(r_+)$. It is possible to find the relationship between the energy e and angular momentum ℓ required that makes this possible and find a general rule that describes the angular velocity of such orbits.

First of all, the four-velocity of the particle will be

$$u^\mu = \left(\frac{\mathrm{d}t}{\mathrm{d}\tau}, 0, 0, \frac{\mathrm{d}\phi}{\mathrm{d}\tau}\right) = \left(\frac{\mathrm{d}t}{\mathrm{d}\tau}, 0, 0, \frac{\mathrm{d}t}{\mathrm{d}\tau}\Omega\right) = u^t(1, 0, 0, \Omega) \tag{1.29}$$

Where we defined $\Omega := \frac{\mathrm{d}\phi}{\mathrm{d}t}$: the rate at which ϕ changes with respect to the Schwarzschild time t. Using eq. 1.13a and eq. 1.13b, Ω can be rewritten as

$$\Omega := \frac{\mathrm{d}\phi}{\mathrm{d}t} = \frac{\mathrm{d}\tau}{\mathrm{d}t}\frac{\mathrm{d}\phi}{\mathrm{d}\tau} = \frac{1}{r^2}\left(1 - \frac{2M}{r}\right)\frac{\ell}{e}\,. \tag{1.30}$$

A second equation for $\frac{\ell}{e}$ comes with the restriction that the particle must orbit at the minimum of V_{eff}, from eq. 1.23a

$$r = \frac{\ell^2}{2M}\left[1 + \sqrt{1 - 12\left(\frac{M}{\ell}\right)^2}\right]\,. \tag{1.31}$$

Using eq. 1.20 the derivative of r vanishes and we can write everything as

$$e^2 = \left(1 + \frac{\ell^2}{r^2}\right)\left(1 - \frac{2M}{r}\right)\,. \tag{1.32}$$

Instead of substituting r from eq. 1.31 into eq. 1.32, it is easier to solve eq. 1.31 for $1/\ell^2$ obtaining

$$\frac{1}{\ell^2} = \frac{1}{Mr} - \frac{3}{r^2}\,, \tag{1.33}$$

and then use it to rewrite eq. 1.32 as

$$\frac{e^2}{\ell^2} = \left(\frac{1}{\ell^2} + \frac{1}{r^2}\right)\left(1 - \frac{2M}{r}\right) = \left(\frac{1}{Mr} - \frac{3}{r^2} + \frac{1}{r^2}\right)\left(1 - \frac{2M}{r}\right) = \frac{1}{Mr}\left(1 - \frac{2M}{r}\right)^2$$

$$\frac{\ell}{e} = \sqrt{Mr}\left(1 - \frac{2M}{r}\right)^{-1} \tag{1.34}$$

We can finally substitute eq. 1.34 into eq. 1.30 to get

$$\Omega^2 = \frac{M}{r^3} \tag{1.35}$$

that gives the angular velocity observed from infinity of a particle in a circular orbit. With the value of Ω found in eq. 1.35 we can find the normalization of the four-velocity defined in 1.29.

$$-1 = \mathbf{u}\cdot\mathbf{u} = g_{\nu\mu}u^\nu u^\mu = (u^t)^2\left[-\left(1-\frac{2M}{r}\right)+r^2\Omega^2\right]$$
$$(u^t)^2 = \left[1-\frac{2M}{r}-\frac{M}{r}\right]^{-1}$$
$$u^t = \left(1-\frac{3M}{r}\right)^{-1/2}$$

Therefore, we have

$$u^\mu = \left(1-\frac{3M}{r}\right)^{-1/2}\left(1,0,0,\sqrt{\frac{M}{r^3}}\right) \tag{1.36}$$

1.6.2 General Shapes and Precession

To complete the discussion on bound orbit we can have a look at a more general case, where $V_{\text{eff}} < \mathcal{E} < 0$. If we want to characterize the shape of the orbit, as always restricted to the xy plane, we need to express ϕ as a function of r. To do so we can use eq. 1.13b and eq. 1.20 and rewrite them respectively as

$$\frac{\mathrm{d}\phi}{\mathrm{d}\tau} = \frac{\ell}{r^2} \tag{1.37a}$$
$$\frac{\mathrm{d}r}{\mathrm{d}\tau} = \pm\sqrt{e^2-\left(1+\frac{\ell^2}{r^2}\right)\left(1-\frac{2M}{r}\right)}\,. \tag{1.37b}$$

This time we had no reason to keep one sign or the other in eq. 1.37b as the radius can either increase or decrease. Dividing 1.37b into 1.37a gives

$$\frac{\mathrm{d}\phi}{\mathrm{d}r} = \pm\frac{\ell}{r^2}\left[e^2-\left(1+\frac{\ell^2}{r^2}\right)\left(1-\frac{2M}{r}\right)\right]^{-1/2} \tag{1.38}$$

The function $\phi(r)$ can be found simply by integrating the right-hand side. The result can be expressed in terms of elliptic functions but not in a very enlightening way for those not familiar with them[2].

An interesting parameter to study is the *precession*, defined as

$$\delta\phi_{\text{prec}} := \Delta\phi - 2\pi \tag{1.39}$$

To define $\Delta\phi$ consider the turning points P_1 and P_2 in Figure 1.5. *One orbit* is complete when the particle starts from the inner turning point, P_1, and gets back to it. We can equivalently consider P_2 as a starting and ending point. $\Delta\phi$ is the angle swept during one orbit. It's also useful to notice that the angle swept in one orbit is twice the angle swept between P_1 and P_2, thus we can rewrite $\Delta\phi$ as

$$\Delta\phi = \int_{P_1}^{P_2}\frac{\mathrm{d}\phi}{\mathrm{d}r}\mathrm{d}r = 2\ell\int_{r_1}^{r_2}\frac{1}{r^2}\left[e^2-\left(1+\frac{\ell^2}{r^2}\right)\left(1-\frac{2M}{r}\right)\right]^{-1/2}\mathrm{d}r \tag{1.40}$$

[2] **hartle2021gravity**.

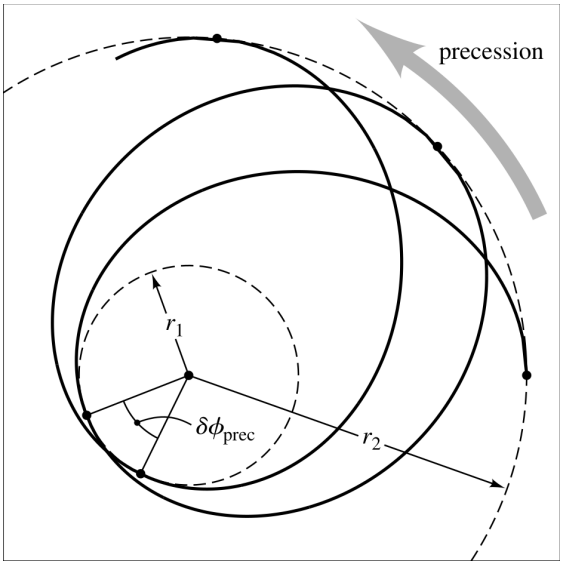

Figure 1.6: Example of precession. Starting from an outer turning point one can trace the orbit ending up at different turning point, therefore sweeping an angle greater than 2π. **hartle2021gravity**.

We used the positive solution from eq. 1.37b as we chose to integrate from the inner turning point P_1 to the outer one P_2 that, respectively correspond to a radius r_1 and r_2 where $r_1 < r_2$. By the definition of the turning points, r_1 and r_2, the integral we need to compute is between the two zeros of the denominator contained in square brackets. To check the correspondence with the Newtonian case we can solve the integral in 1.40 neglecting the r^{-3} term and remembering the definition of $\mathcal{E}$ from eq. 1.21:

$$\Delta\phi = 2\ell \int_{r_1}^{r_2} \frac{1}{r^2} \left[\mathcal{E} - \frac{\ell^2}{r^2} + \frac{2M}{r} \right]^{-1/2} \mathrm{d}r$$

Making the substitution $u = 1/r$ and using the root of the denominator as the bounds of integration we get

$$\Delta\phi = 2 \int_{u_2}^{u_1} \frac{\mathrm{d}u}{\sqrt{(u_1 - u)(u - u_2)}} = 2\pi \qquad \forall u_1 \neq u_2 \tag{1.41}$$

where $u_{1/2} = \frac{1}{r_{1/2}}$. The integral is π for every u_1 and u_2, and therefore the precession for an orbit predicted by Newtonian mechanics will always be 0.

1.7 Light Ray Orbits

As we have introduced in eq. 1.14 and 1.15, the trajectory of a light ray, similarly to the one of a massive particle, has the quantities e and ℓ that are conserved. We can therefore restrict the motion of the light ray to the xy plane as we did with massive particle and use e and ℓ to write the four-velocity as

$$u^\mu = \left(\frac{\mathrm{d}t}{\mathrm{d}\lambda}, \frac{\mathrm{d}r}{\mathrm{d}\lambda}, 0, \frac{\mathrm{d}\phi}{\mathrm{d}\lambda}\right) = \left(e\left(1-\frac{2M}{r}\right)^{-1}, \frac{\mathrm{d}r}{\mathrm{d}\lambda}, 0, \frac{\ell}{r^2}\right).$$

The only difference lies, as described in eq. 1.16b, in the normalization of $\mathbf{u}$, that is $\mathbf{u}\cdot\mathbf{u} = 0$. So, with the same intent we had when we found eq. 1.20, we can write

$$0 = g_{\nu\mu}u^\nu u^\mu = -\left(1-\frac{2M}{r}\right)^{-1} e^2 + \left(1-\frac{2M}{r}\right)^{-1}\left(\frac{\mathrm{d}r}{\mathrm{d}\lambda}\right)^2 + \frac{\ell^2}{r^2}$$

and then rearrange to get

$$e^2 = \left(\frac{\mathrm{d}r}{\mathrm{d}\lambda}\right)^2 + \ell^2\, W_{\text{eff}}(r)\,. \tag{1.42}$$

Here we defined another effective potential, one that acts on light rays only, as

$$W_{\text{eff}}(r) = \frac{1}{r^2}\left(1-\frac{2M}{r}\right). \tag{1.43}$$

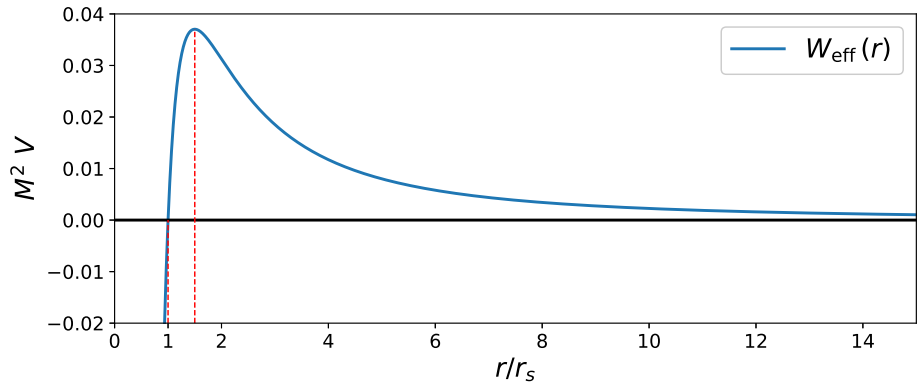

Figure 1.7: Effective potential for light rays, W_{eff}, described in eq. 1.43. We can see the maximum ar $r = 3M = 1.5r_s$ and that the peak of $M^2\ W_{\text{eff}}$ is at $1/27 \simeq 0.037$.

This new potential can be studied, again, by taking the derivative of it with respect to r. We find out the there is one stationary point at $r = 3M$ representing the maximum of the function, as we can also see from Figure 1.7. This is therefore an unstable point, the value of the potential at the maximum is

$$W_{\text{eff}}(3M) = \frac{1}{27M^2}\,.$$

It's interesting to notice that, unlike in the massive particle case, the effective potential W_{eff} is independent of l. Looking at eq. 1.42 we can also rewrite it as

$$\frac{1}{b^2} := \frac{e^2}{\ell^2} = \frac{1}{\ell^2}\left(\frac{\mathrm{d}r}{\mathrm{d}\lambda}\right)^2 + W_{\text{eff}}(r)\,. \tag{1.44}$$

where we defined $b = |\ell/e|$. Here we can use the fact the geodesic is invariant under an affine parameter renormalization to ignore the $1/\ell^2$ in front of the derivative of the radius and understand that only the ratio $\frac{\ell}{e}$ holds physical significance in the massless case.

To see what b is, let's consider a particle approaching the massive object from far away. In this case we will use Cartesian coordinates and say that the massive object is at the origin while the particle starts from a position $(x,\, d)$, refer to figure 1.8.

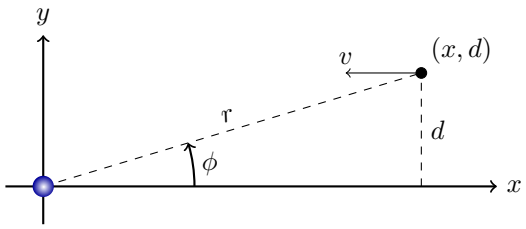

Figure 1.8: Visual representation of a photon approaching the massive object with an impact parameter d.

If we evaluate b in this scenario, considering $r \gg r_s$ and $r \gg d$, we find out that

$$b = \left|\frac{\ell}{e}\right| = \left|r^2\frac{\mathrm{d}\phi}{\mathrm{d}\lambda}\left(1-\frac{2M}{r}\right)^{-1}\frac{\mathrm{d}\lambda}{\mathrm{d}t}\right| \simeq \left|r^2\frac{\mathrm{d}\phi}{\mathrm{d}r}\right| \simeq \left|r^2\frac{\mathrm{d}}{\mathrm{d}r}\left(\frac{d}{r}\right)\right| = d\,.$$

We can then interpret b as the *impact parameter* for a light ray at infinity.

The shape of the orbit, determined by evaluating $\frac{\mathrm{d}r}{\mathrm{d}\lambda}$ from eq. 1.8, is therefore fully characterized by the value of b.

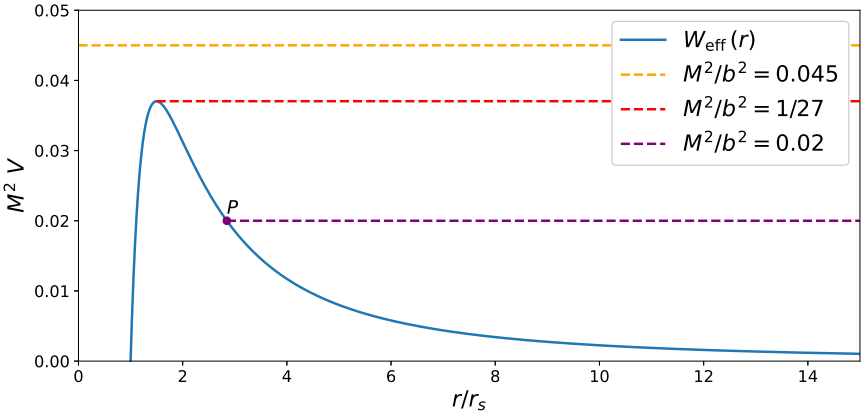

Figure 1.9: Effective potential for light rays W_{eff}, described in eq. 1.43. Different values of the impact parameter b give raise to 3 different type of orbits.

Playing around with the possible values of b, because of the shape of W_{eff}, we can recognize 3 different types of orbits, that are shown in Figure 1.9:

- $b < 3\sqrt{3}M$ (yellow dashed line): in this case the light ray doesn't have an impact parameter big enough and can surpass the potential barrier falling towards the center of the massive object;
- $b = 3\sqrt{3}M$ (red dashed line): This represents an edge case where the light ray can theoretically maintain a circular orbit at the unstable stationary point;
- $b > 3\sqrt{3}M$ (purple dashed line): Here, the light ray has a sufficiently large impact parameter, allowing it to approach the massive object and, upon reaching the turning point P, continue its trajectory back to infinity. This results in a deflection of the light ray's path.

1.8 Deflection of Light

The phenomenon of light deflection, briefly mentioned earlier, is particularly interesting in terms of measurable effects. This effect is, for example, visible in distant stars whose light is deflected by the sun and then observed from the earth.

To find the deflection it is useful to first express ϕ as a function of r. We can rewrite eq. 1.15b and eq. 1.44 as

$$\frac{1}{\ell}\frac{\mathrm{d}\phi}{\mathrm{d}\lambda} = \frac{1}{r^2} \tag{1.45a}$$

$$\frac{1}{\ell}\frac{\mathrm{d}r}{\mathrm{d}\lambda} = \sqrt{\frac{1}{b^2} - W_{\text{eff}}}\,. \tag{1.45b}$$

Dividing eq. 1.45b into 1.45a and recalling the complete expression of W_{eff} from eq. 1.43 we get

$$\frac{\mathrm{d}\phi}{\mathrm{d}r} = \frac{1}{r^2}\left[\frac{1}{b^2} - \frac{1}{r^2}\left(1 - \frac{2M}{r}\right)\right]^{-1/2}\,. \tag{1.46}$$

Looking at Figure 1.10 we can see the deflected ray in thick dashed line spanning an angle $\Delta\phi$ (if we consider it coming from infinity and going back to infinity). A non-deflected ray on the other hand will span an angle of π. The deflection angle we are interested in is therefore the one labeled as $\delta\phi_{\text{def}}$ and is calculated by doing

$$\delta\phi_{\text{def}} = \Delta\phi - \pi \tag{1.47}$$

In the Figure 1.10, r_1 represents the turning point, the point where the light is closer to the massive object (refer to Figure 1.9). Most importantly in this case, r_1 cuts the trajectory in half. We can then evaluate half the angle angle spanned by integrating eq. 1.46 from $r = r_1$ to $r = \infty$. Consequently, the full angle spanned by the deflected light ray will be

$$\Delta\phi = 2\int_{r_1}^{\infty} \frac{1}{r^2}\left[\frac{1}{b^2} - \frac{1}{r^2}\left(1 - \frac{2M}{r}\right)\right]^{-1/2} \mathrm{d}r \tag{1.48}$$

remembering from Figure 1.9 that r_1 is measured when the light ray is in P and $1/b^2 = W_{\text{eff}}(r_1)$

In the integral in 1.48 we can make the substitution $w = b/r$ to rewrite it as

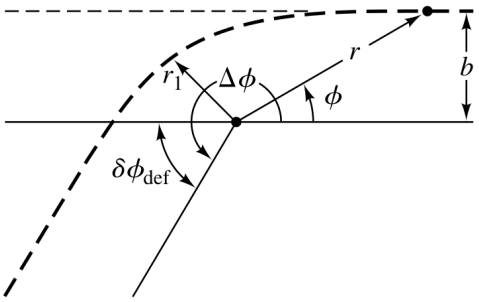

Figure 1.10: Deflected ray, in a thick dashed line, against the non-deflected trajectory, in thin dashed line. A non-deflected ray that goes from right to left (infinitely far) would span an angle of π. The deflected ray instead spans an angle of $\Delta\phi$.
From **hartle2021gravity** *page 211, Figure 9.10*

$$\Delta\phi = 2\int_o^{w_1}\left[1 - w^2\left(1 - \frac{2M}{b}w\right)\right]^{-1/2} \mathrm{d}w \tag{1.49}$$

where w_1 is the value at which the square bracket vanishes. Using eq. 1.47 and eq. 1.11 we can numerically evaluate the integral for different values of b. The result is shown in Figure 1.11.

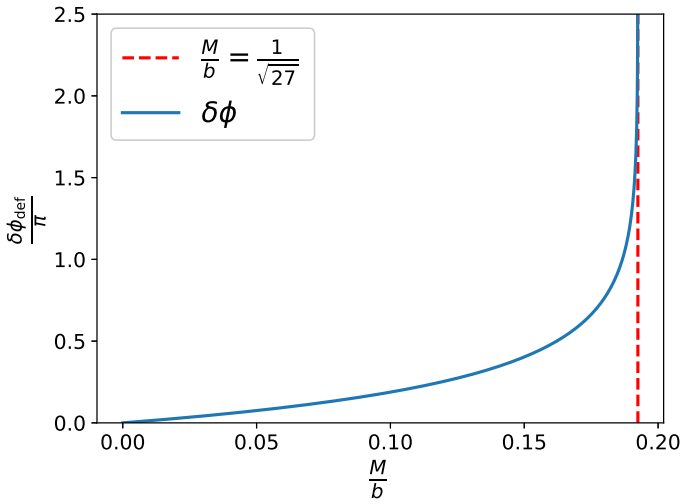

Figure 1.11: Deflection of a light ray because of the gravitational field of a massive object. As $1/b^2 \to 27M^2$ the light ray trajectory gets closer to a circular orbit, and the ray can turn around the massive object multiple times before going back to infinity.

Chapter 2

Simulations

As we have seen in the previous chapter, the Schwarzschild metric describes the geometry of spacetime around a spherically symmetric, non-rotating black hole. Even though it is one of the simplest solutions to the Einstein field equations, the orbits of particles, in general, are not described by closed form solutions.

In this chapter we will build a program in `C` that numerically integrates the equations of motion. The program will allow us to study more complex geodesics and better understand how they differ from the Newtonian case.

2.1 Equations of motion

Recalling the results of the previous chapter we can rewrite the equation for the radial motion 1.28, together with the equations for ϕ and t that come directly from the conservation of angular momentum and energy per rest mass unit, respectively eq. 1.13b and 1.13a.

$$\begin{cases} \dfrac{1}{2}\left(\dfrac{\mathrm{d}r}{\mathrm{d}\tau}\right)^2 = \mathcal{E} - V_{\text{eff}}(r) & \text{(2.1a)} \\ \dfrac{\mathrm{d}\phi}{\mathrm{d}\tau} = \dfrac{l}{r^2} & \text{(2.1b)} \\ \dfrac{\mathrm{d}t}{\mathrm{d}\tau} = \dfrac{e}{1-2M/r} & \text{(2.1c)} \end{cases}$$

Where V_{eff} is the effective potential defined in eq. 1.22 and $\mathcal{E} = \frac{e^2-1}{2}$.

To avoid numerical problems, we will keep geometrized units and express everything in unit of the Schwarzschild radius $r_s = 2M$:

$$r = r_s\hat{r} \qquad \tau = r_s\hat{\tau} \qquad t = r_s\hat{t} \qquad \ell = r_s\hat{\ell} \tag{2.2}$$

The system of equations 2.1 can be rewritten as

$$\begin{cases} \dfrac{\mathrm{d}\hat{r}}{\mathrm{d}\hat{\tau}} = \pm\sqrt{2\mathcal{E} - 2V_{\text{eff}}} & \text{(2.3a)} \\ \dfrac{\mathrm{d}\phi}{\mathrm{d}\hat{\tau}} = \dfrac{\hat{\ell}}{\hat{r}^2} & \text{(2.3b)} \\ \dfrac{\mathrm{d}t}{\mathrm{d}\hat{\tau}} = \sqrt{2\mathcal{E}+1}\left(\dfrac{\hat{r}}{\hat{r}-1}\right) & \text{(2.3c)} \end{cases}$$

The effective potential becomes

$$V_{\text{eff}} = \frac{1}{2}\left(\frac{\hat{\ell}^2}{\hat{r}^2} - \frac{1}{\hat{r}} - \frac{\hat{\ell}^2}{\hat{r}^3}\right). \tag{2.4}$$

The condition on the angular momentum ℓ for the existence of a stable orbits is $\ell > \sqrt{12}M$ and becomes $\hat{\ell} > \sqrt{3}$. The stationary points of V_{eff} from eq. 1.22 are

$$\hat{r}_{\substack{\min\\\max}} = \hat{\ell}^2\left(1 \pm \sqrt{1 - \frac{3}{\hat{\ell}^2}}\right) \qquad \text{for} \quad \hat{\ell} > \sqrt{3} \tag{2.5a}$$

$$\hat{r}_{\text{ISCO}} = 3 \qquad \text{for} \quad \hat{\ell} = \sqrt{3} \tag{2.5b}$$

Where $\hat{r}_{\substack{\min\\\max}}$ respectively represent a local minimum and maximum of the effective potential. The system in 2.3 can be solved numerically with a fourth-order `Runge-Kutta` method. The initial conditions that determine the orbit are $\hat{\ell}$, $\mathcal{E}$ and a compatible starting radius $\hat{r}_0$ (refer to Figure 1.5).

To find the range of r that the particle can explore we need to study when the argument of the square root in eq. 2.3a is positive. In general, we need to solve a cubic equation

$$\frac{\mathrm{d}\hat{r}}{\mathrm{d}\hat{\tau}} = 0 \quad \Rightarrow \quad \mathcal{E} - V_{\text{eff}} = 0 \quad \Rightarrow \quad \hat{r}^3 - \hat{\ell}^2\hat{r}^2 + \hat{\ell}^2 - 2\mathcal{E}\hat{r} - \hat{\ell}^2 = 0\,. \tag{2.6}$$

All the possible scenarios are resumed in Table 2.1.

$\hat{\ell}$	$\mathcal{E}$	$\hat{r}$	Scenario
$[0,\ \sqrt{3}]$	$[0,\ \infty]$	$(1,\ \infty)$	depends on the sign
$[0,\ \sqrt{3}]$	$[-\frac{1}{2},\ 0]$	$(1,\ r_e)$	infall
$(\sqrt{3},\ 2]$	$[0,\ \infty]$	$(1,\ \infty)$	depends on the sign
$(\sqrt{3},\ 2]$	$[V_{\max},\ 0]$	$(1,\ r_2)$	infall
$(\sqrt{3},\ 2]$	$[V_{\min},\ V_{\max}]$	$(r_1,\ r_2)$	bound orbit
$(\sqrt{3},\ 2]$	$[-\frac{1}{2},\ V_{\min}]$	$(1,\ r_e)$	infall
$(2,\infty)$	$[V_{\max},\ \infty]$	$(1,\ \infty)$	depends on the sign
$(2,\infty)$	$[0,\ V_{\max}]$	$(r_1,\ \infty)$	unbound orbit
$(2,\infty)$	$[V_{\min},\ V_{\min}]$	$(r_1,\ r_2)$	bound orbit
$(2,\infty)$	$[-\frac{1}{2},\ V_{\min}]$	$(1,\ r_e)$	infall

Table 2.1: Possible scenarios for the motion of a particle in the Schwarzschild spacetime.

In the table we referred to the local maximum and minimum of the effective potential calculated in $r_{\substack{\min\\\max}}$ as $V_{\min}$ and $V_{\max}$ respectively. Instead of solving the cubic equation analytically, the limiting radii can be calculated using the bisect method and imposing that 2.6 must be 0

between 1 and $r_{\min}$ for r_e, between $r_{\min}$ and $r_{\max}$ for r_1 and between $r_{\max}$ and ∞ (1000 in our case) for r_2.

2.2 Infalls

Similarly to the previous chapter, we can start with a radial infall scenario, where $\hat{\ell} = 0$, $\mathcal{E} = 0$.

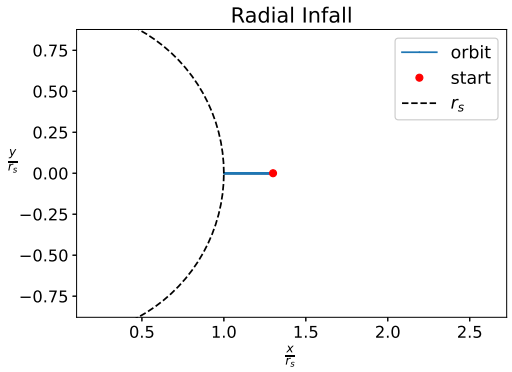

Figure 2.1: Plot of the orbit of a particle in radial infall ($\hat{\ell} = 0$ and $\mathcal{E} = 0$).

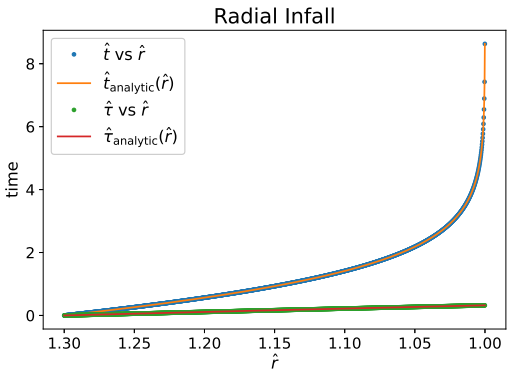

Figure 2.2: Proper time against Schwarzschild time with respect of the radius of a particle falling towards $r = r_s$.

The orbit plot is not the most interesting, but the time plot shows that the numerical integration is working correctly, as the results are consistent with eq. 1.26 and 1.27 found analytically in the previous chapter.

By integrating numerically with this program, we can visualize some more complex infalls.

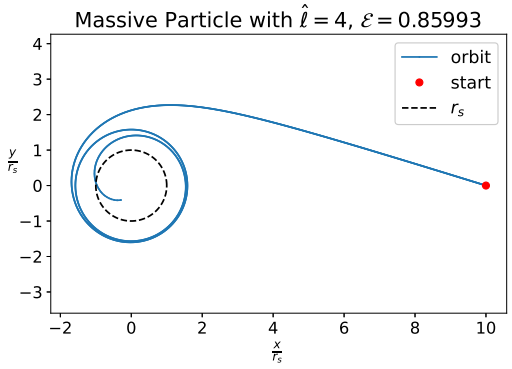

Figure 2.3: The particle starts at $\hat{r}_0 = 10$ ($\hat{r}_{\max} \simeq 1.6$) and has an energy slightly greater than $V_{\text{eff}}(r_{\max}) \simeq 0.859927$. As a result the radial velocity decreases when the particle passes through $\hat{r} = \hat{r}_{\max}$.

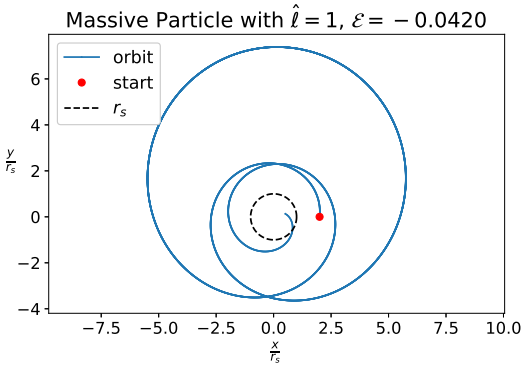

Figure 2.4: V_{eff} is monotonic because $\ell < \sqrt{3}$. The particle starts at $\hat{r} = 2$ with its radial velocity directed outward; however, due to its negative energy $\mathcal{E}$, the particle will not be able to escape.

2.3 Bound Orbits

2.3.1 Circular Orbits

We can also study bound orbits when considering particles with $\hat{\ell} > \sqrt{3}$ and $\mathcal{E} < \min\{V_{\max}, 0\}$. As seen in section 1.6.1 in the previous chapter we have a circular orbit only if $\mathcal{E} = V_{\text{eff}}(\min)$. In this case holds the relation (from eq. 1.35)

$$\Omega^2 = \frac{1}{2\hat{r}^3} \qquad \text{where} \qquad \Omega := \frac{\mathrm{d}\phi}{\mathrm{d}\hat{t}}\,. \tag{2.7}$$

In Figure 2.5 we can see the orbit of a particle with $\hat{\ell} = 3$ and $\mathcal{E} = V_{\text{eff}}(r_{\min}) \simeq -1.478 \times 10^{-2}$. Figure 2.6 shows the normalized residuals of the angular velocity Ω computed from ϕ and $\hat{t}$ obtained during the simulation against the expected value.

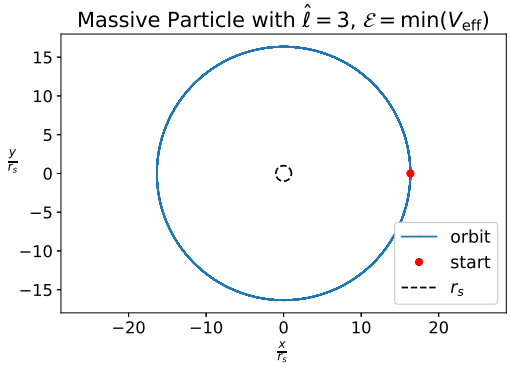

Figure 2.5: The perfectly circular orbit of a particle with $\hat{\ell} = 3$ and $\mathcal{E} = V_{\text{eff}}(r_{\min}) \simeq -1.478 \times 10^{-2}$. The particle starts at $\hat{r} = r_{\min} \simeq 16.35$ and the radius is left unchanged.

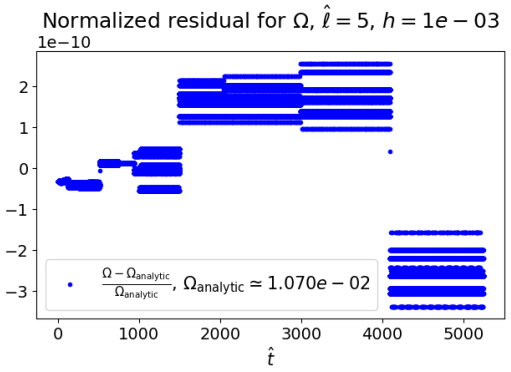

Figure 2.6: The residual of the calculated angular velocity Ω from the data of ϕ and $\hat{t}$ and the expected value calculated from the initial radius $\Omega_{\text{analytic}} = 1/(2\hat{r}_{\min})$.

The relative error is of order 10^{-10} with a time increment $h = 0.001$, we can conclude that the numerical integration is correctly implemented and most of the error comes from the finite precision.

2.3.2 Precession

Therefore, we can proceed with confidence to study bound orbits of different shapes. Recall from eq. 1.39 and 1.40 that, for a bound orbit where the two turning points are labeled $r_1 < r_2$, the precession is given by

$$\delta\phi = 2\int_{r_1}^{r_2} \left(2\mathcal{E} + \frac{2M}{r} - \frac{l^2}{r^2} + \frac{2Ml^2}{r^3}\right)^{-1/2} \mathrm{d}r \; - 2\pi\,. \tag{2.8}$$

If we make the substitution $r = 1/u$ and use the definition of $\mathcal{E} = \frac{e^2-1}{2}$, we can rewrite the integral as

$$\delta\phi = 2\int_{u_2}^{u_1} \frac{1}{\sqrt{2\mathcal{E} + 2Mu - l^2u^2 + 2Ml^2u^3}}\,\mathrm{d}u \; - 2\pi\,. \tag{2.9}$$

The bounds of the integral are $u_2 = 1/r_2 < u_1 = 1/r_1$. Under the square root we have a cubic equation in u with coefficients

$$\text{coefficients} \qquad a = 2Ml^2, \quad b = -l^2, \quad c = 2M, \quad d = 2\mathcal{E} \tag{2.10}$$

$$\text{roots} \qquad u_1,\ u_2,\ u_3\,. \tag{2.11}$$

Since all the coefficients are real, the roots of the equation must either consist of three real roots or one real root and a pair of complex conjugate roots. Given that we are considering bound orbits, we know that two real roots must exist. Therefore, we can infer that all three roots are real and can be labeled such that $u_1 < u_2 < u_3$.

The Wikipedia article *Precession of orbits*[1] shows that, knowing the roots in 2.11, the integral in 2.9 can be expressed in terms of the complete elliptic integral of the first kind $K(m)$

$$\delta\phi = 2\int_{u_2}^{u_1} \frac{1}{\sqrt{(u-u_1)(u-u_2)(u-u_3)}}\,\mathrm{d}u \;- 2\pi = \frac{K(m)}{\sqrt{r_s(u_3-u_1)}} - 2\pi\,. \tag{2.12}$$

Where K and m are respectively defined as

$$K(m) = \int_0^{\pi/2} \frac{\mathrm{d}\theta}{\sqrt{1 - m\sin^2\theta}}\,, \qquad m = \frac{u_2 - u_1}{u_3 - u_1} \tag{2.13}$$

and can be numerically solved in python using the `scipy.special.ellipk` function.

We can now compare the precession of a particle computed from the numerical data of the simulation with the expected value calculated from the initial conditions with the library for elliptic integrals.

Figure 2.7 2.8 ref ref shows some examples of bound orbits with different values of $\hat{\ell}$ and $\mathcal{E}$.

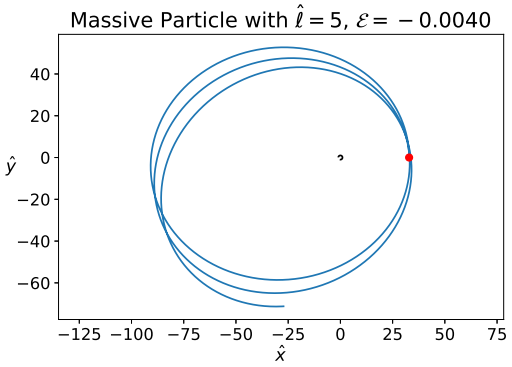

Figure 2.7: $\hat{\ell} = 5$ produces a V_{eff}

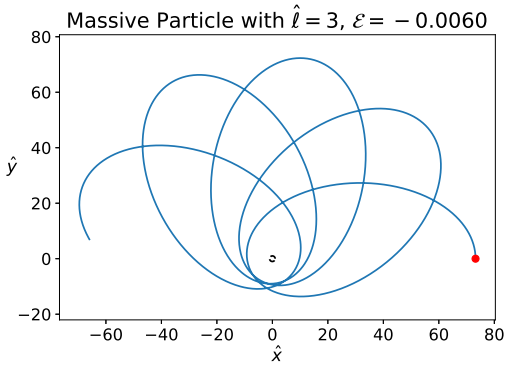

Figure 2.8

[1] **enwiki:1242536958**.

Conclusions

Appendix A

Geometrized Units

In general relativity the constants $G \simeq 6.674\,30 \times 10^{-11}\mathrm{N\,m^2\,kg^{-2}}$ and $c = 299\,792\,458\mathrm{m/s}$ appears quite often, so it is useful to redefine our units of measurements to cancel them out. Let's take the Schwarzschild line element as an example

$$\mathrm{d}s^2 = -\left(1 - \frac{2GM}{c^2 r}\right)(c\mathrm{d}t)^2 + \left(1 - \frac{2GM}{c^2 r}\right)^{-1}\mathrm{d}r^2 + r^2(\mathrm{d}\theta^2 + \sin^2\theta\mathrm{d}\phi^2)\,. \tag{A.1}$$

Time always appears next to the speed of light, ct. This is effectively as if we were measuring time with the distance that light can cover in t seconds.

The mass M is measured in kg in S.I. units. If we multiply it by G and divide by c^2 we get

$$\left[\frac{GM}{c^2}\right] = \frac{\mathrm{N\,m^2\,kg^{-2}\,kg}}{\mathrm{m^2\,s^{-2}}} = \frac{\mathrm{N}}{\mathrm{kg}}\mathrm{s}^2 = \mathrm{m}\,.$$

So, in a less intuitive way, we can measure the mass as a distance too.

Substituting $\hat{t} = ct$ and $\hat{M} = \frac{GM}{c^2}$ in eq. A.1 gives

$$\mathrm{d}s^2 = -\left(1 - \frac{2\hat{M}}{r}\right)\mathrm{d}\hat{t}^2 + \left(1 - \frac{2\hat{M}}{r}\right)^{-1}\mathrm{d}r^2 + r^2(\mathrm{d}\theta^2 + \sin^2\theta\mathrm{d}\phi^2)\,.$$

In this way we went from a $\mathcal{LMT}$(Length Mass Time) units system, to an $\mathcal{L}$ one. Since it will be clearly said when this convention, loosely referred to as $G = c = 1$, is in use we will omit the *hat* in the new defined variables.

To go back to $\mathcal{LMT}$ units we just need to substitute back $t \to ct$ and $M \to \frac{GM}{c^2}$, being extra careful on cases like the speed, that is derived from time and therefore inherits a $1/c$ factor.

Table A.1 shows some typical masses values expressed in geometrical units.

	S.I. units	Geometrized units
Mass of the Earth	5.97×10^{24} kg	4.43 mm
Mass of the Sun	1.99×10^{30} kg	1.48 km
M87 black hole	$6.5 \times 10^9 M_\odot$	64.2 au

Table A.1: Some common masses of the universe expressed in unit of length.

List of Figures

List of Tables